

STR-MATCH: MATCHING SPATIOTEMPORAL RELEVANCE SCORE FOR TRAINING-FREE VIDEO EDITING

000
001
002
003
004
005 **Anonymous authors**
006 Paper under double-blind review
007
008
009
010
011
012
013
014
015
016
017
018
019
020
021
022
023
024
025
026
027
028
029
030
031
032
033
034
035
036
037
038
039
040
041
042
043
044
045
046
047
048
049
050
051
052
053

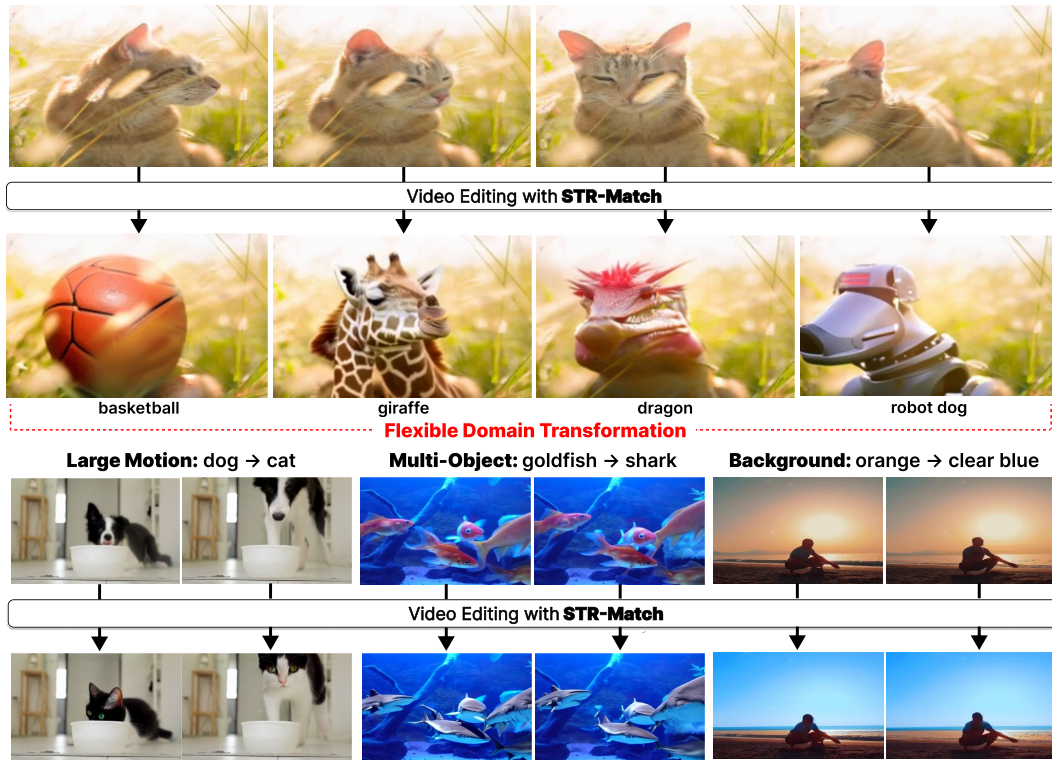


Figure 1: **Generated videos using our proposed algorithm, STR-Match.** Our proposed algorithm, STR-Match, successfully performs flexible domain transformations while preserving the visual information of the source video during the video editing process. It is also applicable to various scenarios, including large motion, multi-object, and background editing.

ABSTRACT

Existing text-guided video editing methods often suffer from temporal inconsistency, motion distortion, and cross-domain transformation error. We attribute these limitations to insufficient modeling of spatiotemporal pixel relevance during the editing process. To address this, we propose STR-Match, a training-free video editing technique that produces visually appealing and temporally coherent videos through latent optimization guided by our novel STR score. The proposed score captures spatiotemporal pixel relevance across adjacent frames by leveraging 2D spatial attention and 1D temporal attention maps in text-to-video (T2V) diffusion models, without the overhead of computationally expensive full 3D attention. Integrated into a latent optimization framework with a latent mask, STR-Match generates high-fidelity videos with strong spatiotemporal consistency, preserving key visual attributes of the source video while remaining robust under significant domain shifts. Our extensive experiments demonstrate that STR-Match consistently outperforms existing methods in both visual quality and spatiotemporal consistency.

054

1 INTRODUCTION

056 Diffusion models (Ho et al., 2020; Song et al., 2021a;b) are the leading framework for high-fidelity
 057 image and video generation using text prompts. Their applications now extend to tasks such as
 058 text-guided image and video editing, where the goal is to generate outputs aligned with target
 059 text prompts while preserving regions consistent with both the source and target prompts in the
 060 original content. Text-guided image editing typically generates a target image using information
 061 extracted during the forward or reconstruction pass of the source image—most commonly via latent
 062 optimization (Parmar et al., 2023; Lee et al., 2025) or attention injection (Cao et al., 2023; Tumanyan
 063 et al., 2023; Hertz et al., 2023), although some methods adopt alternative strategies such as text
 064 embedding interpolation (Kawar et al., 2023; Lee et al., 2024).

065 While text-guided image editing methods have demonstrated impressive editing capabilities, directly
 066 applying them to video editing presents several challenges, including frame inconsistency and
 067 undesired motion change. To achieve strong video editing performance while addressing these issues,
 068 many prior works (Qi et al., 2023; Jeong & Ye, 2024; Cong et al., 2024; Yang et al., 2025a) leverage
 069 pretrained text-to-image (T2I) models augmented with additional components. Some other recent
 070 works (Meral et al., 2024; Yatim et al., 2024; Zhang et al., 2025b; Bai et al., 2024) adopt text-to-video
 071 (T2V) models to tackle these problems. However, these methods still suffer from the same issues and
 072 exhibit degraded performance in challenging scenarios (e.g., large domain shifts).

073 These limitations in text-guided video editing stem from inadequate modeling of spatiotemporal
 074 pixel relevance, which is crucial for producing natural and coherent video content. To address
 075 these challenges, we introduce STR-Match, a training-free algorithm that generates videos via latent
 076 optimization guided by a novel STR score. The STR score, defined as the multiplicative combination
 077 of self- and temporal-attention maps, captures spatiotemporal pixel relevance across adjacent frames
 078 by combining 2D spatial and 1D temporal attention from a text-to-video (T2V) diffusion model,
 079 without relying on costly full 3D attention maps. This joint formulation offers greater flexibility
 080 than treating the attention components separately, as it relaxes excessive constraints and facilitates
 081 finding optimal solutions for video editing. Integrated into a latent optimization framework with
 082 a masking strategy, STR-Match produces temporally consistent, high-fidelity outputs, effectively
 083 handling challenging editing cases and maintaining the key visual attributes of the source.

084 Our primary contributions are summarized as follows:

- 085 • We introduce STR-Match, a novel training-free text-guided video editing approach built upon
 086 pretrained T2V diffusion models. It matches spatiotemporal information in the generation
 087 process (target latents) to that of the forward process (source latents) via latent optimization,
 088 optionally incorporating a latent masking strategy for improved preservation of source content.
 089 This design addresses key limitations of existing methods stemming from insufficient modeling
 090 of spatiotemporal pixel relevances.
- 091 • To obtain spatiotemporal information, we propose the STR score, a spatiotemporal pixel
 092 relevance score that combines self- and temporal-attention maps without requiring full 3D
 093 attention maps. The STR score also enables flexible optimization, resulting in enhanced overall
 094 video quality.
- 095 • Through extensive experiments on various video editing tasks, we demonstrate that STR-
 096 Match outperforms existing training-free video editing approaches both quantitatively and
 097 qualitatively. STR-Match generates temporally coherent, high-fidelity videos with flexible
 098 domain transformations, while preserving the visual integrity of the source video. It consistently
 099 outperforms prior methods in these aspects.

100

2 RELATED WORKS

101

2.1 TEXT-TO-VIDEO DIFFUSION MODEL

102 Recent works (Chen et al., 2024; Wang et al., 2024) build on diffusion models by extending pretrained
 103 text-to-image (T2I) architectures. These methods commonly introduce lightweight 1D temporal
 104 modules into 2D spatial backbones, enabling efficient video generation while preserving the visual
 105 priors learned from T2I models. While previous T2V models such as VideoCrafter2 (Chen et al., 2024)

108 and LaVie (Wang et al., 2024) extend pretrained T2I architectures by inserting lightweight temporal
 109 modules into 2D spatial backbones, more recent approaches aim to capture richer spatiotemporal
 110 pixel relevances through full 3D attention. Building on advances in efficient attention computation
 111 frameworks such as xFormers (Lefauzeux et al., 2022) and FlashAttention (Dao et al., 2022), the
 112 latest T2V models (Yang et al., 2025b; Peng et al., 2025) incorporate full 3D attention into their
 113 architectures. For example, CogVideoX (Yang et al., 2025b) and Open-Sora-2.0 (Peng et al., 2025)
 114 adopt 3D autoencoding architectures with integrated full 3D attention, leveraging FlashAttention to
 115 enable efficient attention computation. These methods typically aim to optimize the computation
 116 of attention outputs while avoiding the explicit construction of full 3D attention maps, which are
 117 computationally expensive and thus impractical to use directly.

118 2.2 TRAINING-FREE VIDEO EDITING METHODS

120 **T2I-based video editing methods** With the rapid progress of image editing works (Cao et al.,
 121 2023; Hertz et al., 2023; Tumanyan et al., 2023; Parmar et al., 2023; Lee et al., 2025; Si et al., 2025;
 122 Kawa et al., 2023; Lee et al., 2024), recent works (Qi et al., 2023; Jeong & Ye, 2024; Cong et al.,
 123 2024; Yang et al., 2025a) leverage pretrained T2I models with additional components to complement
 124 frame consistency. FateZero (Qi et al., 2023) manipulates attention maps using binary masks from
 125 cross-attention and improves temporal consistency by warping middle-frame features during diffusion.
 126 Ground-A-Video (Jeong & Ye, 2024) leverages external models—such as GLIGEN (Li et al., 2023a),
 127 RAFT (Teed & Deng, 2020), ZoeDepth (Bhat et al., 2023), and ControlNet (Zhang et al., 2023)—to
 128 guide attention modulation with attention maps. FLATTEN (Cong et al., 2024) manipulates attention
 129 maps to follow patch trajectories derived from optical flow (Teed & Deng, 2020), aiming to maintain
 130 frame consistency. VideoGrain (Yang et al., 2025a) modulates both self- and cross-attention to
 131 address multi-grain video editing tasks, relying on external methods (Tumanyan et al., 2023; Cong
 132 et al., 2024) to enhance frame consistency. Although these T2I-based methods have demonstrated
 133 strong editing capabilities, they still struggle from temporal inconsistency and motion distortion.
 134 Moreover, many of these approaches rely on attention injection, which can disrupt the computational
 135 graph of the pretrained model and often lead to visual artifacts.

136 **T2V-based video editing methods** In contrast to T2I-based approaches, several recent meth-
 137 ods (Meral et al., 2024; Yatim et al., 2024; Zhang et al., 2025b; Bai et al., 2024) leverage pretrained
 138 T2V models to address temporal consistency in the video editing task. For example, DMT (Yatim
 139 et al., 2024) utilizes a pretrained T2V model and introduces a feature descriptor extracted from inter-
 140 mediate layers to guide latent optimization for motion preservation. MotionFlow (Meral et al., 2024)
 141 incorporates losses from cross-, self-, and temporal-attention, along with mask-based manipulation,
 142 to preserve motion information in the source video. Zhang et al. (Zhang et al., 2025b) extracts motion
 143 patterns using temporal modules and applies a frame-to-frame consistency loss during generation.
 144 These approaches utilize latent optimization, which preserves the pretrained model’s computation
 145 graph, allowing for smoother outputs with fewer visual artifacts. However, these methods primar-
 146 ily focus only on motion guidance, which often leads to modifications in unwanted regions (e.g.,
 147 backgrounds). While UniEdit (Bai et al., 2024) uses attention injection for appearance and motion
 148 editing, the foreground and background often become visually decoupled, resulting in incoherent
 149 video outputs.

150 3 PRELIMINARY

151 **Text-to-video diffusion model** We summarize the basic concept of pretrained text-to-video diffusion
 152 models as we use the models to perform text-guided video editing. The key components of text-
 153 to-video model are an encoder $\text{Enc}(\cdot)$, a decoder $\text{Dec}(\cdot)$, and a noise prediction network $\epsilon_\theta(\cdot)$.
 154 Encoder spatially and temporally compresses a video vector $\mathbf{x} \in \mathbb{R}^{F \times H \times W \times 3}$ to a latent vector
 155 $\mathbf{z}_0 \in \mathbb{R}^{f \times h \times w \times c}$, and decoder decompresses the latent vector to the video vector. The noise prediction
 156 network learns the distribution of latent vectors \mathbf{z}_0 , and is trained to minimize following objective
 157 function:

$$\mathbb{E}_{\mathbf{z}_0, \mathbf{c}, t, \epsilon} [\|\epsilon_\theta(\mathbf{z}_t, t, \mathbf{c}) - \epsilon\|_2^2], \quad (1)$$

158 where \mathbf{z}_0 denotes the video latent, \mathbf{c} is the corresponding text prompt, t is the diffusion timestep, and
 159 $\mathbf{z}_t = \alpha_t \mathbf{z}_0 + \sigma_t \epsilon$ for $\epsilon \sim \mathcal{N}(0, \mathbf{I})$. α_t and σ_t are predefined constants satisfying $\alpha_0 = 1$, $\sigma_0 = 0$, and
 160 $\sigma_T / \alpha_T \gg 1$.

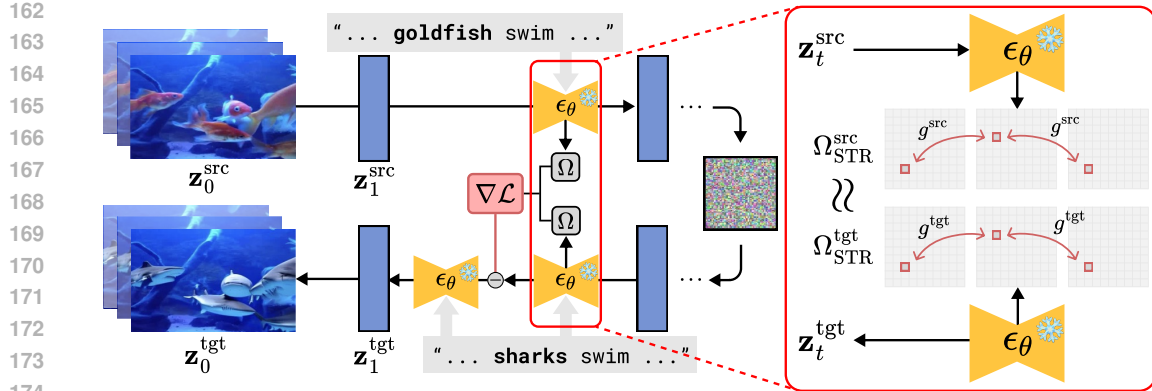


Figure 2: **Illustration of overall STR-Match framework.** We first perform a forward diffusion process, and extract the STR score $\Omega_{\text{STR},t}^{\text{src}}$ from the source video. Then, the target latent is initialized as $\mathbf{z}_T^{\text{tgt}} = \mathbf{z}_T^{\text{src}}$, and during the generation process, we extract the target STR score $\Omega_{\text{STR},t}^{\text{tgt}}$ and optimize the latent $\mathbf{z}_t^{\text{tgt}}$ using a negative cosine similarity between the source and target STR scores. To further preserve unediting regions, we optionally apply a latent mask strategy using a binary mask M .

Attention maps We specifically focus on two key components of text-to-video models: the spatial self-attention map and the temporal-attention map. Spatial self-attention map, whose dimension is $\mathbb{R}^{f \times h \times n \times n}$, captures relevances between pixels within each frame, where f denotes the number of frames, n represents the number of pixels per frame, and h indicates the number of attention heads. For the rest of the paper, we denote $p, q \in \{1, 2, \dots, n\}$ for the spatial location of pixel and $i, j \in \{1, 2, \dots, f\}$ for the frame number. Combining these, $I_i(p)$ represents the pixel at location p in i -th frame. Then, the self-attention map element $\text{Attn}(I_i(p) \rightarrow I_i(q))$ can be interpreted as importance of $I_i(q)$ to $I_i(p)$ in 2D spatial space. Similarly, temporal-attention map, whose dimension is $\mathbb{R}^{n \times h \times f \times f}$, encodes inter-frame relevances for each pixel, and the element $\text{Attn}(I_i(p) \rightarrow I_j(p))$ represents the importance of $I_j(p)$ to $I_i(p)$ in 1D temporal space.

4 METHODS

Many text-guided image editing methods (Cao et al., 2023; Hertz et al., 2023; Tumanyan et al., 2023; Parmar et al., 2023; Si et al., 2025) manipulate attention maps, demonstrating that modeling pixel relevances is crucial for effective image editing. Likewise, we expect that spatiotemporal pixel relevances in videos are essential for effective video editing. To this end, we propose the STR score, which captures spatiotemporal pixel relevance across frames by leveraging self- and temporal-attention maps from both U-Net and DiT-based T2V models. It is an aggregation of bidirectional pixel relevances across adjacent frames, efficiently capturing spatiotemporal information and enabling the extraction of key visual attributes from the source video. By integrating the STR score into a latent optimization framework, as illustrated in Figure 2, we enable video editing that preserves source content while achieving high visual quality with flexible domain shifts.

4.1 STR SCORE: SPATIOTEMPORAL RELEVANCE SCORE

U-Net based T2V Models To quantitatively represent relevance between two pixels $I_i(p)$ and $I_j(q)$ in spatiotemporal space, we define two functions: bidirectional relevance $g(\cdot, \cdot)$, and directional relevance $g(\cdot \rightarrow \cdot)$. The directional relevance $g(I_i(p) \rightarrow I_j(q))$ quantifies the importance of $I_j(q)$ to $I_i(p)$ in spatiotemporal space, and intuitively, it is expected to be large if both the importance of $I_j(p)$ to $I_i(p)$ and $I_j(q)$ to $I_j(p)$ are high, or the importance of $I_i(q)$ to $I_i(p)$ and $I_j(q)$ to $I_i(q)$ are high. From this motivation, we define directional relevance between $I_j(q)$ given $I_i(p)$ as

$$g(I_i(p) \rightarrow I_j(q)) := \text{Attn}(I_i(p) \rightarrow I_j(p)) \text{Attn}(I_j(p) \rightarrow I_j(q)) + \text{Attn}(I_i(p) \rightarrow I_i(q)) \text{Attn}(I_i(q) \rightarrow I_j(q)), \quad (2)$$

for $\text{Attn}(\cdot \rightarrow \cdot)$ defined in Section 3. The bidirectional relevance $g(I_i(p), I_j(q))$ extends the directional relevance by considering the connection between $I_i(p)$ and $I_j(q)$ in both directions, as illustrated in Figure 3. Specifically, it is defined as a sum of the importance of $I_j(q)$ to $I_i(p)$ and the

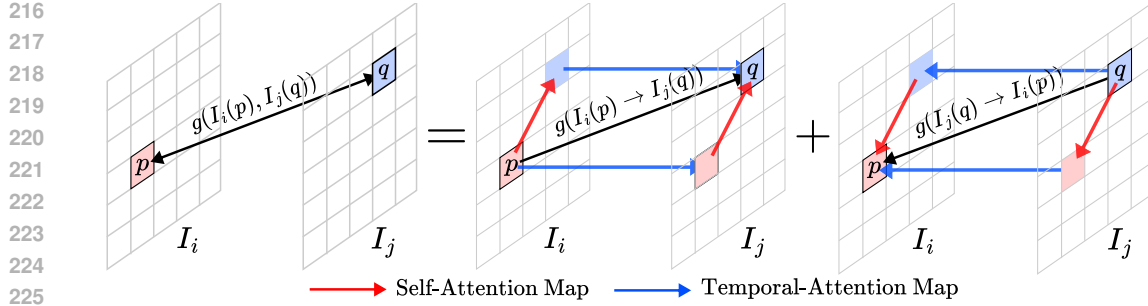


Figure 3: **Illustration of STR score.** (Left) The bidirectional pixel relevance in the spatiotemporal space $g(I_i(p), I_j(q))$ is computed by summing two directional relevance scores along opposite directions. (Right) Each figure illustrates the directional pixel relevance, $g(I_i(p) \rightarrow I_j(q))$ and $g(I_j(q) \rightarrow I_i(p))$, both of which are computed solely through pixel-wise multiplication of self- and temporal-attention maps.

importance of $I_i(p)$ to $I_j(q)$:

$$g(I_i(p), I_j(q)) := g(I_i(p) \rightarrow I_j(q)) + g(I_j(q) \rightarrow I_i(p)). \quad (3)$$

Notably, the bidirectional relevance is fully computed from self- and temporal-attention maps without requiring any additional training or models.

To capture spatiotemporal information in the source video—such as motion and structural layout—we aggregate bidirectional pixel relevances across adjacent frames into a unified representation, termed the STR score. The STR score Ω_{STR} , or spatiotemporal pixel relevance, is formally defined as follows:

$$\Omega_{\text{STR}}(i, p, q) = \sum_{j \in \mathcal{N}(i)} g(I_i(p), I_j(q)), \quad (4)$$

where $\mathcal{N}(i)$ is a set of neighboring frame numbers to the i -th frame.

DiT-based T2V Models Recent DiT-based T2V models often bypass the explicit computation of attention maps, which makes it challenging to obtain spatiotemporal relevances, $\text{Attn}(I_i(p) \rightarrow I_j(p))$ and $\text{Attn}(I_j(p) \rightarrow I_i(q))$. To address this limitation, we introduce pseudo self-attention and temporal-attention maps that efficiently approximate these relevances. The query and key matrices generally have the shape $(h, f \times n, c)$, where c denotes the channel dimension and the remaining symbols follow the notation in Section 3. For computation, we reshape the query and key tensors to two forms— $(f \times h, n, c)$ and $(n \times h, f, c)$ —to compute pseudo self- and temporal-attention maps via dot-product and softmax. This yields a pseudo self-attention map of shape (f, h, n, n) and a pseudo temporal-attention map of shape (n, h, f, f) , which are directly employed in Equation (2). Our formulation enables the efficient computation of STR scores across diverse T2V models, independent of their architectures, without the need to construct full 3D attention maps—a strategy further analyzed in terms of computational complexity in Appendix B.

4.2 OVERALL FRAMEWORK: STR-MATCH

The overall procedure of our method is illustrated in Figure 2 and Algorithm 1. We first solve the forward diffusion process of the source video. During the forward process, we extract STR scores $\Omega_{\text{STR},t}^{\text{src}}$ at every timestep and noisy latent $\mathbf{z}_T^{\text{src}}$. Then, starting from $\mathbf{z}_T^{\text{tgt}} = \mathbf{z}_T^{\text{src}}$ as initial point, we perform generation process with latent optimization. For each denoising step, we first optimize the latent variable $\mathbf{z}_t^{\text{tgt}}$, and then solve diffusion process with the optimized latents. The optimization is performed with the following equation:

$$\mathbf{z}_t^{\text{tgt}} \leftarrow \mathbf{z}_t^{\text{tgt}} - \lambda \nabla_{\mathbf{z}_t^{\text{tgt}}} \mathcal{L}_{\text{cos}}(\Omega_{\text{STR},t}^{\text{src}}, \Omega_{\text{STR},t}^{\text{tgt}}), \quad (5)$$

where \mathcal{L}_{cos} is a negative cosine similarity, and λ is a hyperparameter for controlling the guidance strength. The equation is designed to maximize the cosine similarity between the source and target STR scores, encouraging the spatiotemporal pixel relevances in the target video to align with those of source video to promote preservation of spatiotemporal information.

270

Algorithm 1 STR-Match

271

```

1: Input:  $\mathbf{z}_0^{\text{src}}$  (source video),  $p^{\text{src}}$  (source prompt embedding),  $p^{\text{tgt}}$  (target prompt embedding),  $\Phi(\cdot)$  (ODE solver),  $M$  (foreground binary mask, optional)
2: Hyperparameter:  $\lambda$  (coefficient of negative cosine similarity)
3: for  $t = 0$  to  $T - 1$  do
4:    $\epsilon_t^{\text{src}} \leftarrow \epsilon_\theta(\mathbf{z}_t^{\text{src}}, t, p^{\text{src}})$ 
5:   Compute and save  $\Omega_{\text{STR},t}^{\text{src}}$  from  $\epsilon_\theta(\cdot)$ 
6:    $\mathbf{z}_{t+1}^{\text{src}} \leftarrow \Phi(\mathbf{z}_t^{\text{src}}, \epsilon_t^{\text{src}}, t \rightarrow t + 1)$ 
7: end for
8:  $\mathbf{z}_T^{\text{tgt}} \leftarrow \mathbf{z}_T^{\text{src}}$ 
9: for  $t = T$  to 1 do
0:   Compute  $\Omega_{\text{STR},t}^{\text{tgt}}$  from  $\epsilon_\theta(\mathbf{z}_t^{\text{tgt}}, t, [p^{\text{tgt}}; p^{\text{src}}])$ 
1:    $\mathbf{z}_t^{\text{tgt}} \leftarrow \mathbf{z}_t^{\text{tgt}} - \lambda \nabla_{\mathbf{z}_t^{\text{tgt}}} \mathcal{L}_{\text{cos}}(\Omega_{\text{STR},t}^{\text{src}}, \Omega_{\text{STR},t}^{\text{tgt}})$ 
2:    $\epsilon_t^{\text{tgt}} \leftarrow \epsilon_\theta(\mathbf{z}_t^{\text{tgt}}, t, [p^{\text{tgt}}; p^{\text{src}}])$ 
3:    $\mathbf{z}_{t-1}^{\text{tgt}} \leftarrow \Phi(\mathbf{z}_t^{\text{tgt}}, \epsilon_t^{\text{tgt}}, t \rightarrow t - 1)$ 
4:   if  $M$  exists then
5:      $\mathbf{z}_{t-1}^{\text{tgt}} \leftarrow (1 - \text{dilate}(M)) \odot \mathbf{z}_{t-1}^{\text{src}} + \text{dilate}(M) \odot \mathbf{z}_{t-1}^{\text{tgt}}$ 
6:   end if
7: end for
8: Result:  $\mathbf{z}_{\Omega}^{\text{tgt}}$  (target video)

```

291

Since the optimization process preserves the computational graph of the pretrained model, it enables the generation of smooth, high-quality videos while maintaining key visual information from the source. Moreover, since Ω_{STR} is conceptually defined as the element-wise product of self- and temporal-attention maps, it enables more flexible optimization compared to using them independently, thereby further enhancing video quality.

297

Latent mask strategy To better preserve regions that are not intended to be edited (e.g., backgrounds), we mix the optimized latent with the latent obtained during the forward process at the same timestep. For a binary mask M , where values are 1 for regions to be edited and 0 otherwise, and latents $\mathbf{z}_t^{\text{src}}$ obtained during the forward diffusion process of source video, the final target latents are updated as

$$\mathbf{z}_t^{\text{tgt}} \leftarrow (1 - \text{dilate}(M)) \odot \mathbf{z}_t^{\text{src}} + \text{dilate}(M) \odot \mathbf{z}_t^{\text{tgt}}. \quad (6)$$

303

This masking strategy ensures to preserve non-target regions in the source video during editing. The latent binary mask is resized and dilated version of segmentation map of editing region of the source video. The `dilate` function is applied to help flexible shape modification.

306

5 EXPERIMENTS

308

5.1 IMPLEMENTATION DETAILS

310

For U-Net based experiments, STR-Match is implemented using LaVie (Wang et al., 2024) as the pretrained T2V model. For efficient inference, we extract the STR score based on self- and temporal-attention maps, excluding those from the finest resolution. We compare our method against recent training-free video editing algorithms: FateZero (Qi et al., 2023), Ground-A-Video (GAV) (Jeong & Ye, 2024), FLATTEN (Cong et al., 2024), VideoGrain (Yang et al., 2025a), DMT (Yatim et al., 2024), and UniEdit (Bai et al., 2024). For T2I-based methods (FateZero, Ground-A-Video, FLATTEN, VideoGrain), we follow their official implementations. For T2V-based baselines (DMT, UniEdit), we adopt LaVie (Wang et al., 2024) as the pretrained T2V model to ensure a fair comparison. We employ a video segmentation model SAM-Track (Cheng et al., 2023) to obtain binary mask M , and OWL-ViT (Minderer et al., 2022), an object detection model to obtain bounding boxes for Ground-A-Video.

311

For DiT-based experiments, we implement STR-Match using the pretrained CogVideoX-2B (Yang et al., 2025b). To improve computational efficiency during optimization, STR scores are computed using only the first two attention blocks of CogVideoX-2B. We compare our approach with CogVideoX-V2V, a recent training-free video editing method built on the same backbone.



Figure 4: **Qualitative comparisons between STR-Match with LaVie and existing methods.** In each example, STR-Match demonstrates stronger foreground–background texture alignment, higher visual fidelity, better motion alignment, and more flexible shape transformation compared to recent existing methods. Please refer to our HTML-based supplementary material for the edited video results.

All experiments are conducted on a single NVIDIA L40S GPU with 48 GB of memory. We use a fixed hyperparameter $\lambda = 0.01$ and optimize with SGD. For extreme qualitative scenarios (e.g., cat \rightarrow basketball) in the U-Net based setting, we select λ from the range $[0.005, 0.015]$. We set the number of diffusion timesteps to 50 and apply classifier-free guidance (Ho & Salimans, 2021) with a scale of 7.5. A detailed description of the pretrained base models and external models used in implementation is provided in Table 1 of Appendix A.1. Additionally, we provide the results of object deletion/addition and the ablation studies of STR-Match in Appendix D and Appendix E, respectively.

Quantitative evaluation protocol For quantitative evaluation in the U-Net based setting, we collect a total of 54 videos, each consisting of 16 frames, comprising samples from the TGVE dataset (Wu et al., 2023) and additional videos sourced from the Internet¹. We utilize VideoLLaMA3-7B (Zhang et al., 2025a), a pretrained video captioning model, to obtain concise prompts of source videos automatically, and randomly change nouns to construct the corresponding target prompt. We measure four metrics to evaluate the fidelity and faithfulness of the edited videos to source video and target prompt. Frame Consistency (FC) suggested in VBench (Huang et al., 2024) measures the smoothness of videos, leveraging motion priors in the frame interpolation model (Li et al., 2023b). CLIP Similarity (CS) computes the average CLIP score (Hessel et al., 2021) between the target prompt and edited video. BG-LPIPS (BL) calculates the Learned Perceptual Image Patch Similarity (LPIPS) score (Zhang et al., 2018) between masked frames of the source and generated videos, where the mask is 1 for regions to preserve. Motion Error (ME) quantifies the average motion difference between the source and generated videos. It is calculated as the pixel-wise differences of optical flows between each video pair, where the optical flows are obtained using RAFT-Large (Teed & Deng, 2020).

For the DiT-based setting, we use 31 synthesized videos, each containing 17 frames. We compare STR-Match against CogVideoX-V2V using the VE-Bench score (Sun et al., 2025), a comprehensive

¹<https://www.pexels.com>

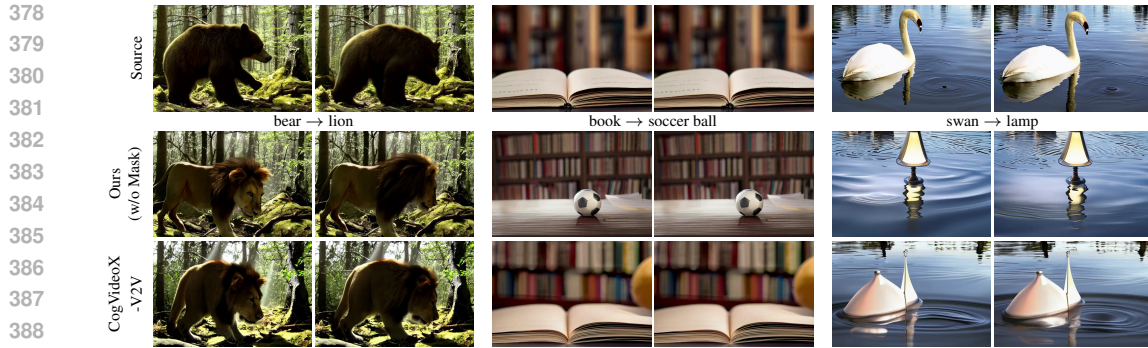


Figure 5: **Qualitative comparisons between STR-Match with CogVideoX and CogVideoX-V2V.** STR-Match demonstrates strong editing capability even in DiT-based settings, outperforming CogVideoX-V2V. In each example, STR-Match performs flexible and effective domain transformation, generating target objects that are natural and faithful to the prompt. In contrast, CogVideoX-V2V either fails to replace the source object or produces results anchored to the source object’s shape, resulting in less realistic outcomes.

metric that assesses video editing quality across multiple dimensions, including frame consistency, text alignment, and fidelity to the source video. In addition, we report VE-Bench results in the U-Net based setting to further validate the effectiveness of our approach.

5.2 QUALITATIVE RESULTS

Key features of STR-Match Figure 1 demonstrates STR-Match’s robust editing performance, highlighting its flexibility in challenging scenarios—such as transforming objects into entirely different categories, handling large motion, performing multi-object editing, and modifying background. For instance, transforming a cat into a basketball or a giraffe demonstrates STR-Match’s ability to faithfully adapt object shapes to target prompts without being overly anchored to the original shape. Moreover, changing a cat into a dragon or a robot dog—objects unlikely to appear in the original scene—illustrates STR-Match’s effective integration of edited elements with the background. These examples emphasize how STR-Match manages domain-shifted objects and significant shape changes, while ensuring the edited elements blend naturally with the background. This combination of flexibility, visual quality, and motion preservation makes STR-Match a powerful tool for diverse video editing tasks.

Comparison to other editing methods Figure 4 compares STR-Match with LaVie to recent video editing baselines, showing that our method achieves sharper visual fidelity, tighter foreground–background texture alignment, and more faithful shape transformations. In the ‘baby → sleeping baby’ case, DMT, UniEdit, and VideoGrain tint the infant while leaving the background gray, whereas STR-Match maintains consistent tonality across the entire frame by capturing spatiotemporal pixel relevance through the STR score. In the ‘lotus → daisy’ example, several baselines either fail to replace the lotus at all or succeed only by unintentionally changing the background. On the other hand, STR-Match successfully replaces the lotus with high fidelity while preserving the background intact. The same trend holds on more dynamic contents. In the ‘zebra → horse’ example, most prior methods either fail to capture the horse’s leg motion (*e.g.*, lifting its leg) or degrade appearance quality, while Ground-A-Video further disrupts scene consistency. In contrast, STR-Match faithfully reproduces the motion with high visual fidelity.

Furthermore, STR-Match demonstrates strong performance even in extreme video editing scenarios. In the ‘cat → basketball’ example, most existing methods fail to transform the cat into a basketball, while DMT generates a basketball at the cost of undesired background changes. Similarly, in the ‘fish → sweet potato’ case, DMT and FLATTEN partially modify the object but suffer from background distortion or low fidelity, and other methods fail to perform the edit. In contrast, STR-Match successfully transforms the object with high visual fidelity while preserving the background. In summary, STR-Match enables high-fidelity, and flexible shape transformation in video editing while preserving spatiotemporal information.

432
 433
 434
 435
 436
 437
 438
 439
 440
 441
 442
 443
 444
 445
 446
 447
 448
 449
 450
 451
 452
 453
 454
 455
 456
 457
 458
 459
 460
 461
 462
 463
 464
 465
 466
 467
 468
 469
 470
 471
 472
 473
 474
 475
 476
 477
 478
 479
 480
 481
 482
 483
 484
 485
 Figure 5 presents a qualitative comparison between STR-Match and CogVideoX-V2V in the DiT-based setting. In the ‘bear → lion’ example, CogVideoX-V2V generates a lion that remains anchored to the shape of the bear, resulting in an unnatural appearance. In contrast, STR-Match produces a lion with a more natural shape and pose. In the ‘book → soccer ball’ and ‘swan → lamp’ cases, CogVideoX-V2V either fails to apply the transformation or yields low-fidelity results, whereas STR-Match successfully performs high-fidelity object transformations. These results demonstrate that STR-Match effectively edits source videos even under the DiT-based setting.

5.3 QUANTITATIVE COMPARISON

We quantitatively evaluate STR-Match with LaVie against existing training-free video editing methods for four metrics: temporal consistency (FC), fidelity to the target prompt (CS), background preservation (BL), and motion preservation from the source video (ME). STR-Match, with and without binary masks, achieves strong performance, as evidenced by its large area in the radar graph shown in Figure 6. Notably, compared to T2I-based editing methods, STR-Match demonstrates superior frame consistency, indicating that the proposed STR score effectively captures spatiotemporal pixel relevances from the T2V model.

Furthermore, when comparing STR-Match with masks to UniEdit (red solid and orange lines), both of which utilize SAM-Track, STR-Match outperforms in all evaluated metrics. In the comparison between STR-Match without masks and DMT (red dashed and green lines), the scores reveal that STR-Match more effectively captures key information from the source video, such as background and motion, while maintaining comparable fidelity. This suggests that the STR score achieves a goldilocks balance—preserving essential details from the source video while maintaining the flexibility required for high-fidelity editing—unlike methods that either over-preserve, reducing fidelity, or under-preserve, diminishing faithfulness.

We further evaluate its performance in both U-Net and DiT-based settings using VE-Bench. STR-Match achieves the highest VE-Bench scores across all compared methods in both settings. Detailed results are provided in Table 2 of Appendix A.1.

6 CONCLUSION

In this work, we propose a novel spatiotemporal modeling approach that relates to key limitations in existing video editing methods—such as frame inconsistency, motion distortion, visual artifacts, and notably, limited performance in challenging settings like large-gap domain shifts. To overcome these challenges, we propose the STR score, a spatiotemporal pixel relevance score that captures essential video attributes. Notably, it is computed solely from the self- and temporal-attention maps of a pretrained text-to-video (T2V) diffusion model, requiring no additional training or external models. By integrating the STR score into a latent optimization framework alongside a latent mask strategy, we introduce STR-Match, a zero-shot, training-free video editing algorithm that is compatible with any T2V model. Extensive experiments show that STR-Match consistently outperforms existing training-free methods across all quantitative metrics. Moreover, it generates videos with substantially improved visual quality, supporting realistic and flexible domain transformation, preserved motion dynamics, and strong temporal consistency. These results demonstrate both the effectiveness and generalizability of STR-Match, establishing it as a new state-of-the-art baseline for training-free text-guided video editing.

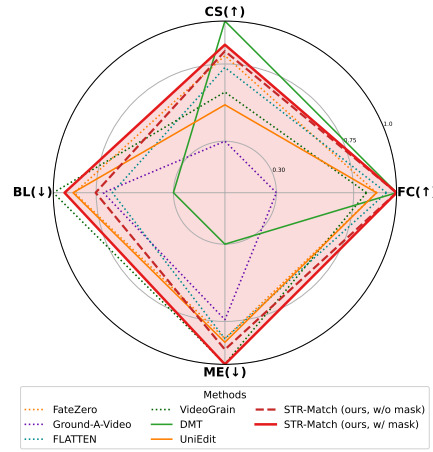


Figure 6: Quantitative comparison between STR-Match with LaVie and existing methods. The solid red line is STR-Match with the binary mask, and the dashed red line is STR-Match without binary mask. The solid lines are T2V-based editing methods, while dotted lines are T2I-based methods. We provide exact metric numbers and analysis in Table 1 of Appendix A.1.

486 REFERENCES
487

488 Jianhong Bai, Tianyu He, Yuchi Wang, Junliang Guo, Haoji Hu, Zuozhu Liu, and Jiang Bian.
489 Unedit: A unified tuning-free framework for video motion and appearance editing. *arXiv preprint*
490 *arXiv:2402.13185*, 2024.

491 Shariq Farooq Bhat, Reiner Birkl, Diana Wofk, Peter Wonka, and Matthias Müller. Zoedepth:
492 Zero-shot transfer by combining relative and metric depth. *arXiv preprint arXiv:2302.12288*, 2023.

493

494 Mingdeng Cao, Xintao Wang, Zhongang Qi, Ying Shan, Xiaohu Qie, and Yinqiang Zheng. Masactrl:
495 Tuning-free mutual self-attention control for consistent image synthesis and editing. In *ICCV*,
496 2023.

497 Haoxin Chen, Yong Zhang, Xiaodong Cun, Menghan Xia, Xintao Wang, Chao Weng, and Ying Shan.
498 Videocrafter2: Overcoming data limitations for high-quality video diffusion models. In *CVPR*,
499 2024.

500

501 Yangming Cheng, Liulei Li, Yuanyou Xu, Xiaodi Li, Zongxin Yang, Wenguan Wang, and Yi Yang.
502 Segment and track anything. *arXiv preprint arXiv:2305.06558*, 2023.

503

504 Yuren Cong, Mengmeng Xu, Christian Simon, Shoufa Chen, Jiawei Ren, Yanping Xie, Juan-Manuel
505 Perez-Rua, Bodo Rosenhahn, Tao Xiang, and Sen He. Flatten: Optical flow-guided attention for
506 consistent text-to-video editing. In *ICLR*, 2024.

507

508 Tri Dao, Dan Fu, Stefano Ermon, Atri Rudra, and Christopher Ré. Flashattention: Fast and memory-
509 efficient exact attention with io-awareness. In *NeurIPS*, 2022.

510

511 Amir Hertz, Ron Mokady, Jay Tenenbaum, Kfir Aberman, Yael Pritch, and Daniel Cohen-Or. Prompt-
512 to-prompt image editing with cross attention control. In *ICLR*, 2023.

513

514 Jack Hessel, Ari Holtzman, Maxwell Forbes, Ronan Le Bras, and Yejin Choi. Clipscore: A reference-
515 free evaluation metric for image captioning. In *EMNLP*, 2021.

516

517 Jonathan Ho and Tim Salimans. Classifier-free diffusion guidance. In *NeurIPS Workshop*, 2021.

518

519 Jonathan Ho, Ajay Jain, and Pieter Abbeel. Denoising diffusion probabilistic models. In *NeurIPS*,
520 2020.

521

522 Ziqi Huang, Yinan He, Jiashuo Yu, Fan Zhang, Chenyang Si, Yuming Jiang, Yuanhan Zhang, Tianxing
523 Wu, Qingyang Jin, Nattapol Chanpaisit, et al. Vbench: Comprehensive benchmark suite for video
524 generative models. In *CVPR*, 2024.

525

526 Hyeonho Jeong and Jong Chul Ye. Ground-a-video: Zero-shot grounded video editing using text-to-
527 image diffusion models. In *ICLR*, 2024.

528

529 Bahjat Kawar, Shiran Zada, Oran Lang, Omer Tov, Huiwen Chang, Tali Dekel, Inbar Mosseri, and
530 Michal Irani. Imagic: Text-based real image editing with diffusion models. In *CVPR*, 2023.

531

532 Hyunsoo Lee, Minsoo Kang, and Bohyung Han. Diffusion-based conditional image editing through
533 optimized inference with guidance. In *WACV*, 2025.

534

535 Junsung Lee, Minsoo Kang, and Bohyung Han. Diffusion-based image-to-image translation by noise
536 correction via prompt interpolation. In *ECCV*, 2024.

537

538 Benjamin Lefauveux, Francisco Massa, Diana Liskovich, Wenhan Xiong, Vittorio Caggiano, Sean
539 Naren, Min Xu, Jieru Hu, Marta Tintore, Susan Zhang, Patrick Labatut, Daniel Haziza, Luca
Wehrstedt, Jeremy Reizenstein, and Grigory Sizov. xformers: A modular and hackable transformer
modelling library. <https://github.com/facebookresearch/xformers>, 2022.

540

541 Yuheng Li, Haotian Liu, Qingyang Wu, Fangzhou Mu, Jianwei Yang, Jianfeng Gao, Chunyuan Li,
542 and Yong Jae Lee. Gligen: Open-set grounded text-to-image generation. In *CVPR*, 2023a.

543

544 Zhen Li, Zuo-Liang Zhu, Ling-Hao Han, Qibin Hou, Chun-Le Guo, and Ming-Ming Cheng. Amt:
545 All-pairs multi-field transforms for efficient frame interpolation. In *CVPR*, 2023b.

540 Tuna Han Salih Meral, Hidir Yesiltepe, Connor Dunlop, and Pinar Yanardag. Motionflow: Attention-
 541 driven motion transfer in video diffusion models. *arXiv preprint arXiv:2412.05275*, 2024.

542

543 Matthias Minderer, Alexey Gritsenko, Austin Stone, Maxim Neumann, Dirk Weissenborn, Alexey
 544 Dosovitskiy, Aravindh Mahendran, Anurag Arnab, Mostafa Dehghani, Zhuoran Shen, et al. Simple
 545 open-vocabulary object detection. In *ECCV*, 2022.

546 Gaurav Parmar, Krishna Kumar Singh, Richard Zhang, Yijun Li, Jingwan Lu, and Jun-Yan Zhu.
 547 Zero-shot image-to-image translation. In *SIGGRAPH*, 2023.

548

549 Xiangyu Peng, Zangwei Zheng, Chenhui Shen, Tom Young, Xinying Guo, Binluo Wang, Hang Xu,
 550 Hongxin Liu, Mingyan Jiang, Wenjun Li, et al. Open-sora 2.0: Training a commercial-level video
 551 generation model in \$200k. *arXiv preprint arXiv:2503.09642*, 2025.

552

553 Chenyang Qi, Xiaodong Cun, Yong Zhang, Chenyang Lei, Xintao Wang, Ying Shan, and Qifeng
 554 Chen. Fatezero: Fusing attentions for zero-shot text-based video editing. In *ICCV*, 2023.

555

556 Qi Si, Bo Wang, and Zhao Zhang. Contrastive learning guided latent diffusion model for image-to-
 557 image translation. *arXiv preprint arXiv:2503.20484*, 2025.

558

559 Jiaming Song, Chenlin Meng, and Stefano Ermon. Denoising diffusion implicit models. In *ICLR*,
 560 2021a.

561

562 Yang Song, Jascha Sohl-Dickstein, Diederik P Kingma, Abhishek Kumar, Stefano Ermon, and Ben
 563 Poole. Score-based generative modeling through stochastic differential equations. In *ICLR*, 2021b.

564

565 Shiqi Sun, Xi Liang, Shuyang Fan, Wei Gao, and Wen Gao. Ve-bench: Subjective-aligned benchmark
 566 suite for text-driven video editing quality assessment. In *AAAI*, 2025.

567

568 Zachary Teed and Jia Deng. Raft: Recurrent all-pairs field transforms for optical flow. In *ECCV*,
 569 2020.

570

571 Narek Tumanyan, Michal Geyer, Shai Bagon, and Tali Dekel. Plug-and-play diffusion features for
 572 text-driven image-to-image translation. In *CVPR*, 2023.

573

574 Yaohui Wang, Xinyuan Chen, Xin Ma, Shangchen Zhou, Ziqi Huang, Yi Wang, Ceyuan Yang, Yinan
 575 He, Jiashuo Yu, Peiqing Yang, et al. Lavie: High-quality video generation with cascaded latent
 576 diffusion models. In *IJCV*, 2024.

577

578 Jay Zhangjie Wu, Xiuyu Li, Difei Gao, Zhen Dong, Jinbin Bai, Aishani Singh, Xiaoyu Xiang,
 579 Youzeng Li, Zuwei Huang, Yuanxi Sun, et al. Cvpr 2023 text guided video editing competition.
 580 *arXiv preprint arXiv:2310.16003*, 2023.

581

582 Xiangpeng Yang, Linchao Zhu, Hehe Fan, and Yi Yang. Videograin: Modulating space-time attention
 583 for multi-grained video editing. In *ICLR*, 2025a.

584

585 Zhuoyi Yang, Jiayan Teng, Wendi Zheng, Ming Ding, Shiyu Huang, Jiazheng Xu, Yuanming Yang,
 586 Wenyi Hong, Xiaohan Zhang, Guanyu Feng, et al. Cogvideox: Text-to-video diffusion models
 587 with an expert transformer. In *ICLR*, 2025b.

588

589 Danah Yatim, Rafail Fridman, Omer Bar-Tal, Yoni Kasten, and Tali Dekel. Space-time diffusion
 590 features for zero-shot text-driven motion transfer. In *CVPR*, 2024.

591

592 Boqiang Zhang, Kehan Li, Zesen Cheng, Zhiqiang Hu, Yuqian Yuan, Guanzheng Chen, Sicong Leng,
 593 Yuming Jiang, Hang Zhang, Xin Li, et al. Videollama 3: Frontier multimodal foundation models
 594 for image and video understanding. *arXiv preprint arXiv:2501.13106*, 2025a.

595

596 Lvmin Zhang, Anyi Rao, and Maneesh Agrawala. Adding conditional control to text-to-image
 597 diffusion models. In *ICCV*, 2023.

598

599 Richard Zhang, Phillip Isola, Alexei A Efros, Eli Shechtman, and Oliver Wang. The unreasonable
 600 effectiveness of deep features as a perceptual metric. In *CVPR*, 2018.

601

602 Xinyu Zhang, Zicheng Duan, Dong Gong, and Lingqiao Liu. Training-free motion-guided video
 603 generation with enhanced temporal consistency using motion consistency loss. *arXiv preprint
 604 arXiv:2501.07563*, 2025b.